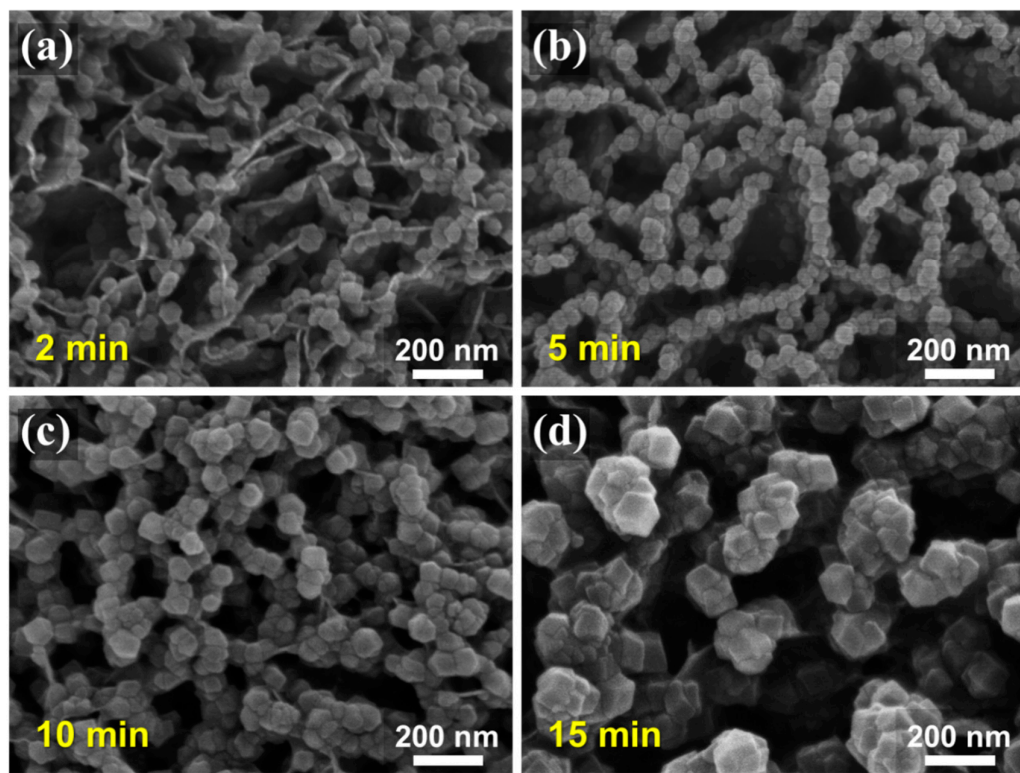


## Supporting Information

### **MOF Template-Derived Carbon Shell Embedded CoP Hierarchical Nanosheet as Bifunctional Catalyst for Overall Water Splitting**

Meijun Liu<sup>a,b</sup>, Fuhao Yang<sup>a</sup>, Jicheng Mei<sup>a,b</sup>, Xu Guo<sup>a</sup>, Huayang Wang<sup>a</sup>, Mengyao He<sup>a</sup>,  
Yuanyang Yao<sup>a</sup>, Haifeng Zhang<sup>a,\*</sup>, Chengbin Liu<sup>b,\*</sup>



**Figure S1.** SEM images of ZIF-67 crystals grown on  $\text{Co}(\text{OH})_2$  nanosheets for (a) 2 min, (b) 5 min, (c) 10 min and (d) 15 min.

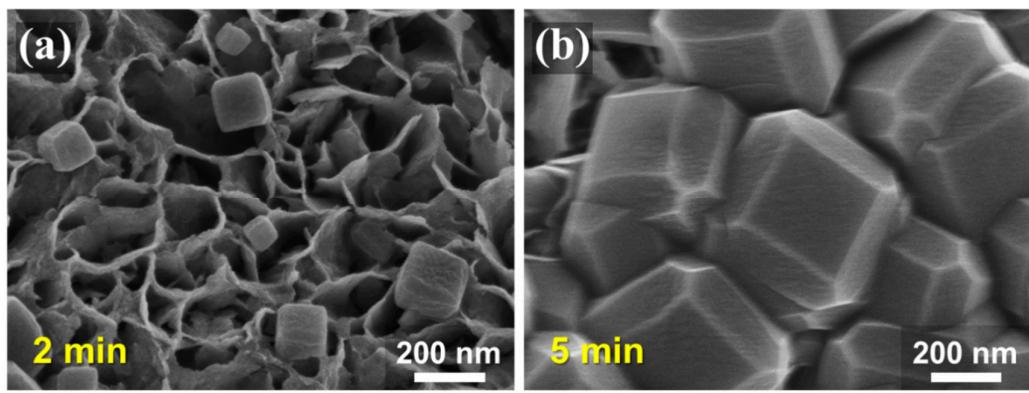


**Figure S2.** SEM images of ZIF-67 crystals grown on  $\text{Co}(\text{OH})_2$  nanosheets for (a) 2 min and (b) 5 min without the acceleration of TEA.

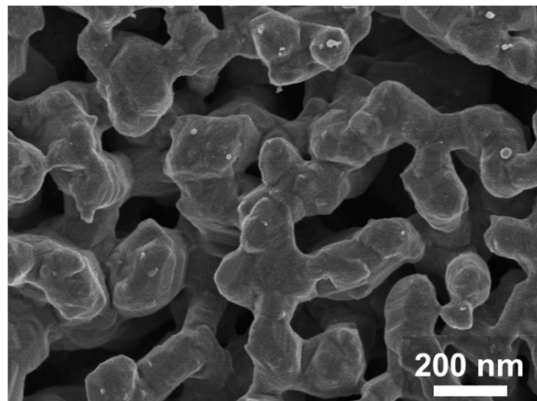


**Figure S3.** SEM image of ZIF-67@Co(OH)<sub>2</sub>-C prepared by directly pyrolytic carbonization of ZIF-67@Co(OH)<sub>2</sub>.

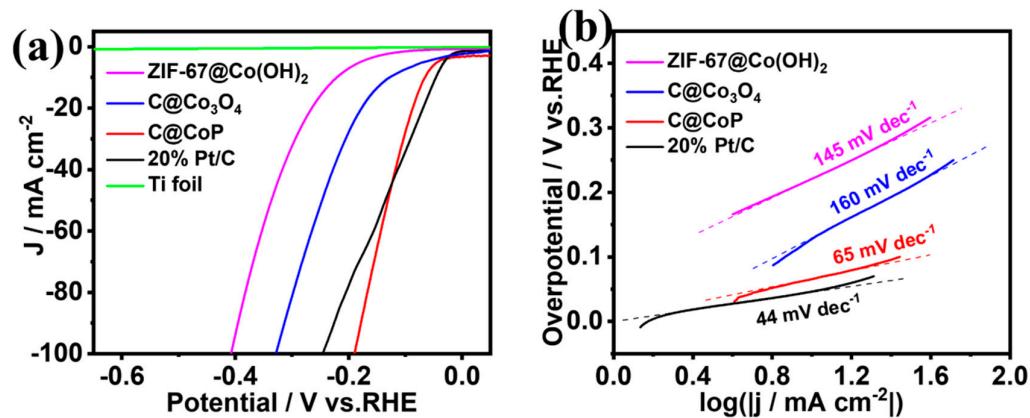


**Figure S4.** (a) HER Polarization curves and corresponding (b) Tafel plots for C@CoP and reference materials.

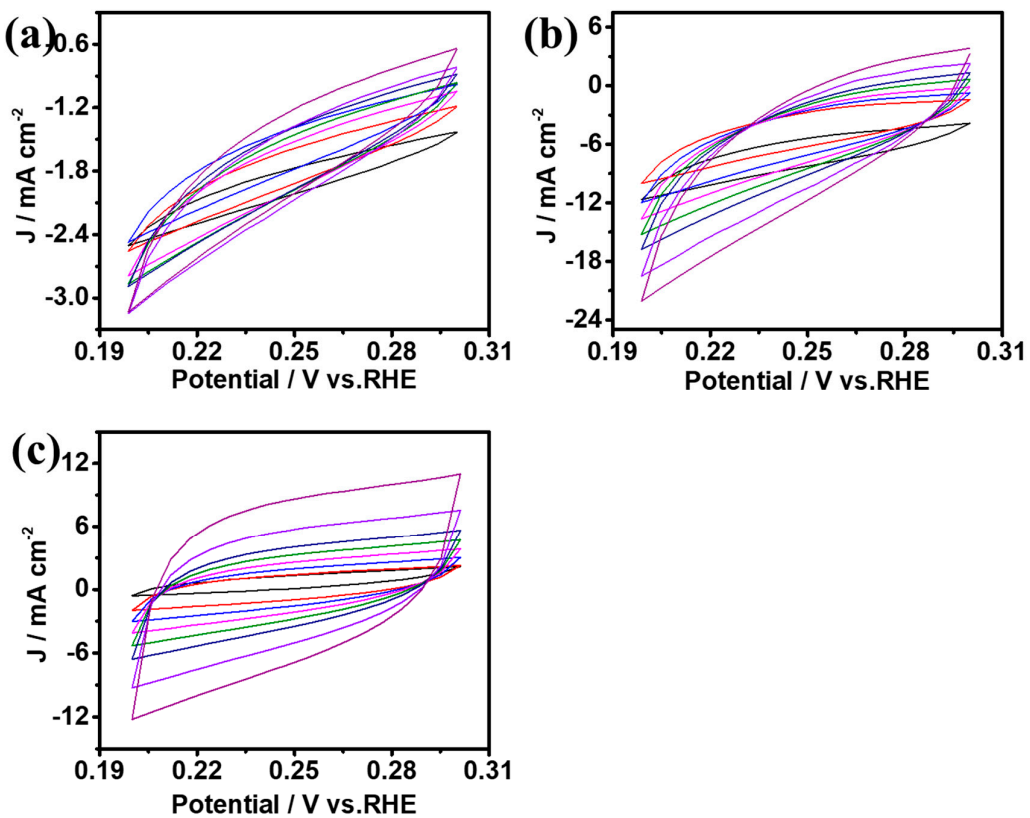


**Figure S5.** CV curves of (a) C@Co<sub>3</sub>O<sub>4</sub>, (b) CoP and (c) C@CoP in the range of 0.2–0.3 V vs.RHE. The curves from inside to outside correspond to the scanning rate of 10, 20, 30, 40, 50, 60, 80 and 100 mV s<sup>-1</sup>, respectively.

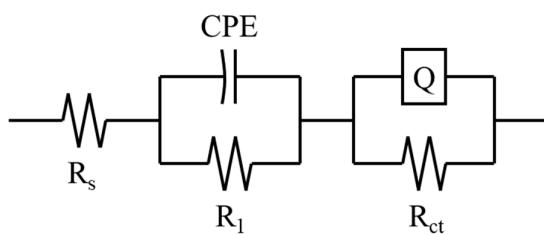


**Figure S6.** Equivalent circuit fitted according to the Nyquist diagram in Figure 5d and Figure 6d .

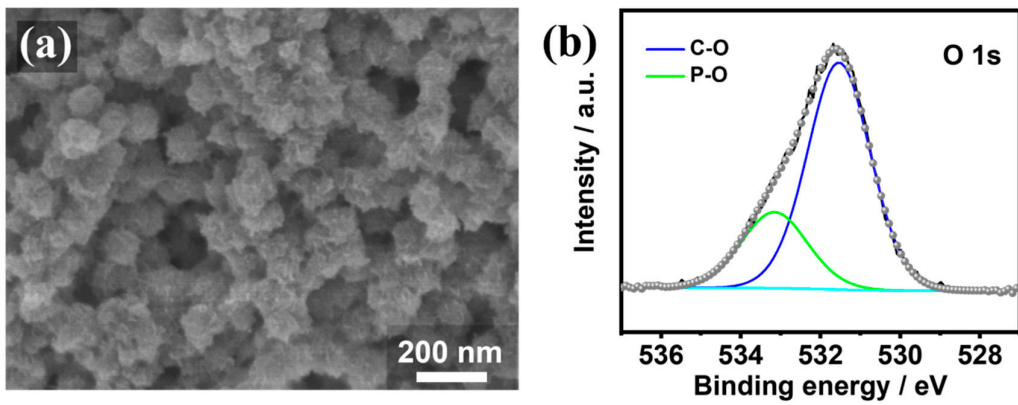


**Figure S7.** (a) SEM image and (b) high-resolution XPS spectra of O 1s of C@CoP

after long term HER test.

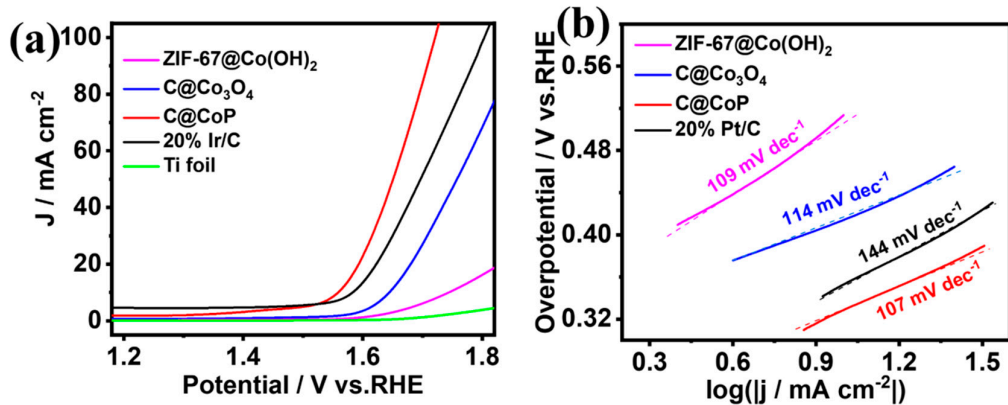


**Figure S8.** (a) OER Polarization curves and corresponding (b) Tafel plots for C@CoP

and reference materials.

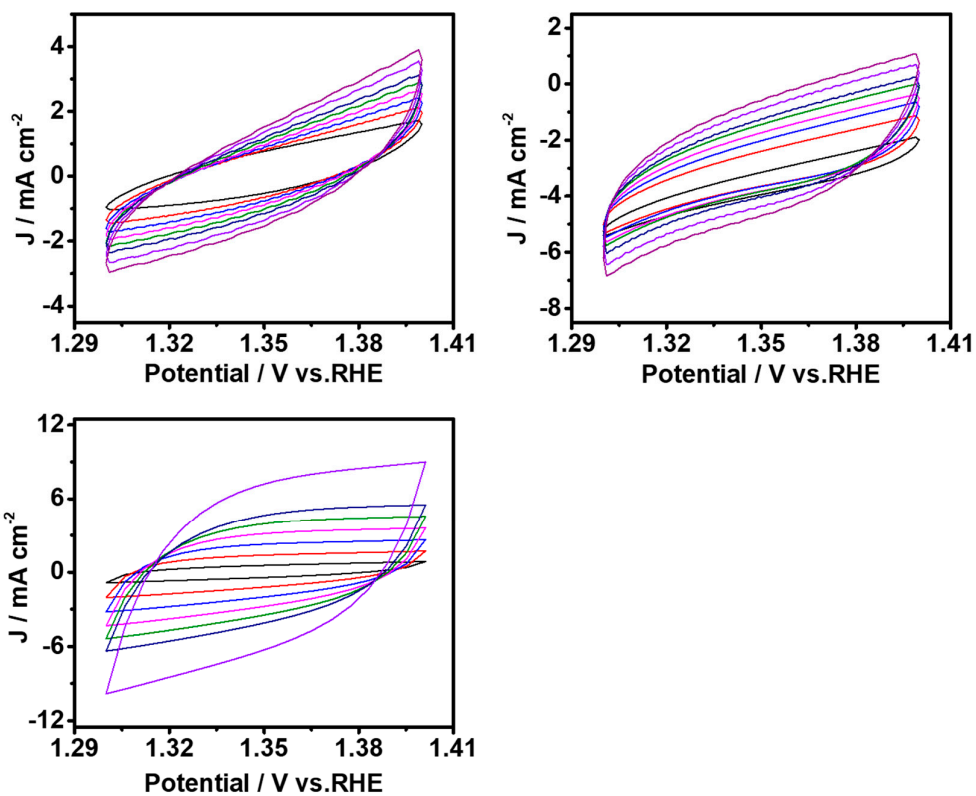


**Figure S9.** CV curves of (a) C@Co<sub>3</sub>O<sub>4</sub>, (b) CoP and (c) C@CoP in the range of 1.3–1.4 V vs.RHE. The curves from inside to outside correspond to the scanning rate of 10, 20, 30, 40, 50, 60, 80 and 100 mV s<sup>-1</sup>, respectively.

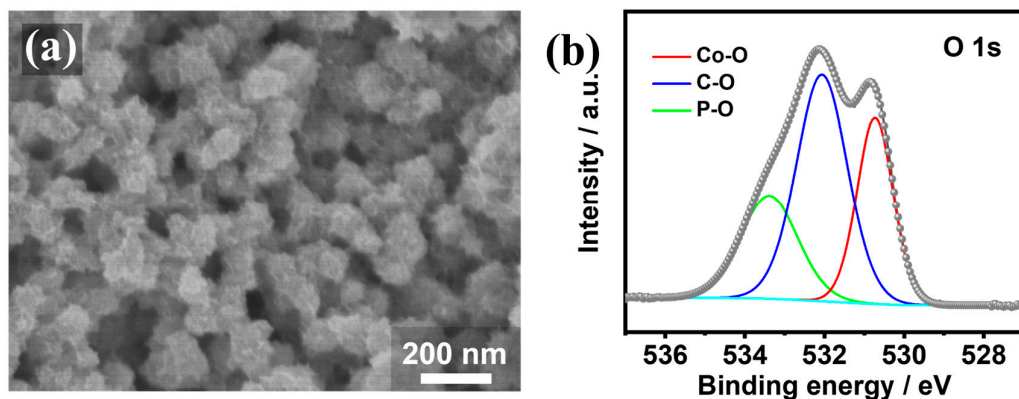


**Figure S10.** (a) SEM image and (b) high-resolution XPS spectra of O 1s of C@CoP after long term OER test.



**Table S1.** Comparison of HER performance for C@CoP with other HER electrocatalysts

Catalyst	Overpotential (mV) at 10 mA/cm <sup>2</sup>	Tafel slope (mV/dec)	Electrolyte	Reference
<b>C@CoP</b>	72	65	1.0 M KOH	This work
<b>Ni-CoP/HPFs</b>	144	62	0.5 M H <sub>2</sub> SO <sub>4</sub>	1
	92	34	1.0 M KOH	
<b>Mn<sub>2</sub>P-Mn<sub>2</sub>O<sub>3</sub>/PNCF</b>	98	46	1.0 M KOH	2
<b>FePx/ Fe-N-C /NPC</b>	75	60	0.5 M H <sub>2</sub> SO <sub>4</sub>	3
	182	132	1.0 M KOH	
<b>CoP/Co-MOF</b>	27	43	0.5 M H <sub>2</sub> SO <sub>4</sub>	4
	34	56	1.0 M KOH	
	49	63	1.0M PBS	
<b>PMA@ZIF-67-C-AT</b>	570	222	0.2M PBS	5
<b>Co<sub>5</sub>Fe<sub>5</sub>-C</b>	165	70.7	1.0 M KOH	6
<b>V-CoP<sub>2</sub>/CC</b>	50	32	0.5 M H <sub>2</sub> SO <sub>4</sub>	7
<b>VCoCOx@NF</b>	63	93	1.0 M KOH	8
<b>Co<sub>2</sub>P/CoP@Co@NCNT</b>	118	46	1.0 M KOH	9
	136	49	0.5 M H <sub>2</sub> SO <sub>4</sub>	

**Table S2.** Electrochemical impedance parameters obtained by fitting the Nyquist plots of Figure 5d to the equivalent circuit model

Catalyst	$R_s$ ( $\Omega$ )	$C$ ( $\text{mF cm}^{-2}$ )	$R_l$ ( $\Omega$ )	Q		$R_{ct}$ ( $\Omega$ )
				$Y_1(\Omega^{-1}s^n)$	n	
C@CoP	1.01	3.89	4.30	$2.56 \times 10^{-3}$	0.480	4.30
CoP	1.17	5.43	5.43	$5.03 \times 10^{-3}$	0.254	5.43
C@Co <sub>3</sub> O <sub>4</sub>	1.22	0.966	22.40	$5.98 \times 10^{-3}$	0.872	22.40

**Table S3.** Comparison of OER performance of C@CoP with other reported electrocatalysts.

Catalyst	Overpotential (mV) at 10 mA/cm <sup>2</sup>	Tafel slope (mV/dec)	Electrolyte	Reference
<b>C@CoP</b>	329	107	1.0 M KOH	This work
<b>Co<sub>5</sub>Fe<sub>5</sub>-C</b>	245	58.2	1.0 M KOH	<sup>6</sup>
<b>W<sub>0.2</sub>Er<sub>0.1</sub>Ru<sub>0.7</sub>O<sub>2-δ</sub></b>	168	66.8	0.5M H <sub>2</sub> SO <sub>4</sub>	<sup>10</sup>
<b>np-Ir/NiFeO</b>	197	29.6	1.0 M KOH	<sup>11</sup>
<b>Mn<sub>2</sub>P-Mn<sub>2</sub>O<sub>3</sub>/PNCF</b>	370	86	1.0 M KOH	<sup>2</sup>
<b>FePx/ Fe-N-C /NPC</b>	325	79	1.0 M KOH	<sup>3</sup>
<b>NiMoP@NiFe-LDH</b>	299	23.3	1.0 M KOH	<sup>12</sup>
<b>V-CoP2/CC</b>	91	40	0.5 M H <sub>2</sub> SO <sub>4</sub>	<sup>7</sup>
<b>VCoCOx@NF</b>	240	65	1.0 M KOH	<sup>8</sup>
<b>Co<sub>2</sub>P/CoP@Co@NCNT</b>	256	46	1.0 M KOH	<sup>9</sup>

**Table S4.** Electrochemical impedance parameters obtained by fitting the Nyquist plots of Figure 6d to the equivalent circuit model

Catalyst	$R_s$	C	$R_l$	Q		$R_{ct}$
	( $\Omega$ )	( $mF\ cm^{-2}$ )	( $\Omega$ )	$Y_l(\Omega^{-1}s^n)$	n	( $\Omega$ )
C@CoP	2.17	4.90	9.66	$6.75 \times 10^{-3}$	0.604	0.59
CoP	2.68	6.75	8.55	$4.45 \times 10^{-3}$	0.968	3.81

**Table S5.** Comparison of overall water splitting performance of C@CoP with recent representative works.

Catalyst	Cell voltage (V) at 10 mA/cm <sup>2</sup>	Electrolyte	Reference
<b>C@CoP</b>	1.63	1.0 M KOH	This work
<b>Mn<sub>2</sub>P-Mn<sub>2</sub>O<sub>3</sub>/PNCF</b>	1.6	1.0 M KOH	<sup>2</sup>
<b>FePx/ Fe-N-C /NPC</b>	1.58	1.0 M KOH	<sup>3</sup>
<b>Ir<sub>1</sub>@Co/NC</b>	1.603	1.0 M KOH	<sup>13</sup>
<b>Co-Fe NPs</b>	1.92	1.0 M KOH	<sup>14</sup>
<b>Fe-NiS<sub>2</sub>/CF</b>	1.722	1.0 M KOH	<sup>15</sup>
<b>O-Ni<sub>0.5</sub>W<sub>0.5</sub>Se<sub>2</sub></b>	1.56	1.0 M KOH	<sup>16</sup>
<b>Co<sub>0.75</sub>Fe<sub>0.25</sub>P</b>	1.63	1.0 M KOH	<sup>17</sup>
<b>Co<sub>2</sub>P/CoP@Co@NCNT</b>	1.6	1.0 M KOH	<sup>9</sup>
<b>Co/Mo<sub>2</sub>C@NC800-2</b>	1.67	1.0 M KOH	<sup>18</sup>

- Pan, Y.; Sun, K.; Lin, Y.; Cao, X.; Cheng, Y.; Liu, S.; Zeng, L.; Cheong, W.-C.; Zhao, D.; Wu, K.; Liu, Z.; Liu, Y.; Wang, D.; Peng, Q.; Chen, C.; Li, Y., Electronic structure and d-band center control engineering over M-doped CoP (M = Ni, Mn, Fe) hollow polyhedron frames for boosting hydrogen production. *Nano Energy* **2019**, *56*, 411-419.
- Wang, X.; Huang, G.; Pan, Z.; Kang, S.; Ma, S.; Shen, P. K.; Zhu, J., One-pot synthesis of Mn<sub>2</sub>P-Mn<sub>2</sub>O<sub>3</sub> heterogeneous nanoparticles in a P, N -doped three-dimensional porous carbon framework as a highly efficient bifunctional electrocatalyst for overall water splitting. *Chemical Engineering Journal* **2022**, *428*.
- Qin, Q.; Jiang, H.; Li, P.; Yuan, B.; Liu, X.; Cho, J., A Tannic Acid-Derived N-, P-Codoped Carbon-Supported Iron-Based Nanocomposite as an Advanced Trifunctional Electrocatalyst for the Overall Water Splitting Cells and Zinc-Air Batteries. *Advanced Energy Materials* **2019**, *9*(5).
- Liu, T.; Li, P.; Yao, N.; Cheng, G.; Chen, S.; Luo, W.; Yin, Y., CoP-Doped MOF-Based Electrocatalyst for pH-Universal Hydrogen Evolution Reaction. *Angew Chem Int Ed Engl* **2019**, *58*(14), 4679-4684.
- Zhao, X.; Zhang, Q.; Huang, X.; Ding, L.; Yang, W.; Wang, C.; Pan, Q., Polyoxometalate@ZIF-67 derived carbon-based catalyst for efficient electrochemical overall seawater splitting and oxygen reduction. *International Journal of Hydrogen Energy* **2022**, *47*(4), 2178-2186.
- Yan, Y.; Han, Y.; Wang, F.; Hu, Y.; Shi, Q.; Diao, G.; Chen, M., Bifunctional electrocatalyst of CoxFey-C for overall water splitting. *Journal of Alloys and Compounds* **2022**, *897*.
- Wang, Y.; Jiao, Y.; Yan, H.; Yang, G.; Tian, C.; Wu, A.; Liu, Y.; Fu, H., Vanadium-Incorporated CoP(2) with Lattice Expansion for Highly Efficient Acidic Overall Water Splitting. *Angew Chem Int Ed Engl* **2022**, *61*(12), e202116233.
- Meena, A.; Thangavel, P.; Nissimagoudar, A. S.; Narayan Singh, A.; Jana, A.; Sol Jeong, D.; Im, H.; Kim, K. S., Bifunctional oxovanadate doped cobalt carbonate for high-efficient overall water splitting in alkaline-anion-exchange-membrane water-electrolyzer. *Chemical Engineering Journal* **2022**, *430*.
- Lu, Z.; Cao, Y.; Xie, J.; Hu, J.; Wang, K.; Jia, D., Construction of Co<sub>2</sub>P/CoP@Co@NCNT rich-interface to synergistically promote overall water splitting. *Chemical Engineering Journal* **2022**, *430*.
- Hao, S.; Liu, M.; Pan, J.; Liu, X.; Tan, X.; Xu, N.; He, Y.; Lei, L.; Zhang, X., Dopants fixation of Ruthenium for boosting acidic oxygen evolution stability and activity. *Nature Communications* **2020**, *11*(1), 5368.
- Jiang, K.; Luo, M.; Peng, M.; Yu, Y.; Lu, Y. R.; Chan, T. S.; Liu, P.; de Groot, F. M. F.; Tan, Y., Dynamic active-site generation of atomic iridium stabilized on nanoporous metal phosphides for water oxidation. *Nat Commun* **2020**, *11*(1), 2701.
- Xiao, L.; Bao, W.; Zhang, J.; Yang, C.; Ai, T.; Li, Y.; Wei, X.; Jiang, P.; Kou, L., Interfacial interaction between NiMoP and NiFe-LDH to regulate the electronic structure toward high-efficiency electrocatalytic oxygen evolution reaction. *International Journal of Hydrogen Energy* **2022**, *47*(15), 9230-9238.
- Lai, W.-H.; Zhang, L.-F.; Hua, W.-B.; Indris, S.; Yan, Z.-C.; Hu, Z.; Zhang, B.; Liu, Y.; Wang, L.; Liu, M.; Liu, R.; Wang, Y.-X.; Wang, J.-Z.; Hu, Z.; Liu, H.-K.; Chou, S.-L.; Dou,

- S.-X., General  $\pi$ -Electron-Assisted Strategy for Ir, Pt, Ru, Pd, Fe, Ni Single-Atom Electrocatalysts with Bifunctional Active Sites for Highly Efficient Water Splitting. *Angewandte Chemie International Edition* **2019**, *58* (34), 11868-11873.
14. Adamson, W.; Bo, X.; Li, Y.; Suryanto, B. H. R.; Chen, X.; Zhao, C., Co-Fe binary metal oxide electrocatalyst with synergistic interface structures for efficient overall water splitting. *Catalysis Today* **2020**, *351*, 44-49.
15. Yu, C.; Huang, H.; Zhou, S.; Han, X.; Zhao, C.; Yang, J.; Li, S.; Guo, W.; An, B.; Zhao, J.; Qiu, J., An electrocatalyst with anti-oxidized capability for overall water splitting. *Nano Research* **2018**, *11* (6), 3411-3418.
16. Singh, M.; Nguyen, T. T.; Balamurugan, J.; Kim, N. H.; Lee, J. H., Rational manipulation of 3D hierarchical oxygenated nickel tungsten selenide nanosheet as the efficient bifunctional electrocatalyst for overall water splitting. *Chemical Engineering Journal* **2022**, *430*.
17. Huang, Y.; Li, M.; Yang, W.; Yu, Y.; Hao, S., 3D ordered mesoporous cobalt ferrite phosphides for overall water splitting. *Science China Materials* **2020**, *63* (2), 240-248.
18. Liu, G.; Wang, K.; Wang, L.; Wang, B.; Lin, Z.; Chen, X.; Hua, Y.; Zhu, W.; Li, H.; Xia, J., A Janus cobalt nanoparticles and molybdenum carbide decorated N-doped carbon for high-performance overall water splitting. *Journal of Colloid and Interface Science* **2021**, *583*, 614-625.

